

INTERCOMPARISON OF WATER VAPOR CALIBRATION CONSTANTS DERIVED FROM IN-SITU AND DISTANT SOUNDINGS FOR A RAMAN-LIDAR OPERATING IN THE AMAZON FOREST

Henrique M. J. Barbosa¹, Diego A. Gouveia¹, Paulo Artaxo¹, Theotonio Pauliquevis², David K. Adams³

¹*Instituto de Física, USP, São Paulo-SP, Brazil*

²*Centro de Ciências Atmosféricas e Espaciais, Unifesp, São Paulo-SP - Brazil*

³*Depto. de Meteorologia, UEA, Manaus-AM - Brazil*

ABSTRACT

Water vapor profiles derived from UV Raman Lidar measurement need to be calibrated. An approach based on the linear fit between the lidar uncalibrated profile and different reference profiles was used to calibrate a lidar system recently deployed to the Amazon forest. For this site, the nearest operational sounding is 30 km away and near a river. Calibration was done using: (1) collocated reference soundings, (2) non-collocated sounding, (3) non-collocated soundings with only standard WMO GTS atmospheric levels. For collocated soundings, the derived constant was 0.681 ± 0.045 (rms) ± 0.040 (inst) g/g. Initial results with no rayleigh or mie scattering correction show values of non-collocated constant to be 30% larger and statistically significant, what forbids the use of these operational sounding for periodic calibration.

1. INTRODUCTION

Recent studies have focused on the complex relation between water vapor variability and deep convection in the tropics. Differently from high latitudes, dynamical constraints are weak (e.g. Coriolis) and perturbations from diabatic heating are transported over long distances [1]. The concentration of water vapor in the tropics is highly variable in both time and space. Its vertical distribution above the boundary layer depends on slow advective processes and on the deep convection's moisture source to the free troposphere. At the same time, deep convection itself is sensitive to the distribution of humidity in the free troposphere, developing more vigorously in humid environments, a positive feedback [2]. Water vapor also plays an important role in the convective available potential energy (CAPE). CAPE depends essentially on the boundary layer humidity, but also on the concentration of water in the free troposphere through virtual temperature effects [3; 4]. On the other hand, CAPE is constantly removed from the atmosphere by convection itself, a negative feedback that works for stabilization of the atmosphere.

From the above discussion, it is clear that observations with high spatial and temporal resolution are necessary for understanding the complex interactions and feedback mechanisms between convection and humidity which occur in meso or smaller scales. However, there are very few such measurements on tropical regions. Indeed, there were important field campaigns in the Amazon that explored some aspects of deep convection, meso scales

systems and clouds microphysics (e.g., WETAMC and TRMM/LBA [6]). These, however, were short-intensive campaigns that do not allow for a climatological perspective.

To overcome this lack of observations, a new experimental site was recently implemented near Manaus-AM, in the Brazilian Amazon Forest. The ACONVEX site will run continuously during the next years applying a synergy of different instruments, as described in section 2.1. This paper focus on the Raman-Lidar system used for measurements of water vapor and aerosol optical properties vertical distributions. Further details about the system is given in section 2.2. For reliable water vapor measurements, lidar profiles were calibrated with collocated soundings dropped during an intensive campaign in September 2011, as described in section 3. The intent of this paper is to compare this collocated calibration with that from operational sounding performed twice a day 30 km away with: (1) only standard atmospheric levels; and (2) full resolution. Section 4 discuss these results and future work.

2. ACCONVEX

A long time series of measurements with high spatial and temporal resolution are necessary for understanding the complex interactions and feedback mechanisms between convection and humidity which occur in meso or smaller scales. As mentioned before, apart from important field campaigns there are very few such measurements in the tropical regions, particularly over the Amazon.

The *Aerosols, Clouds, cONvection EXperiment* (ACONVEX) intends to fill in the gap of a long time series of measurements with high spatial and temporal resolution necessary for understanding the interactions and feedback mechanisms between humidity, convection, clouds and aerosols. It was initially implemented by a partnership between different research projects: AEROCLIMA (Direct and indirect effects of aerosols on climate in Amazonia and Pantanal), CHUVA (Cloud processes of the main precipitation systems in Brazil: A contribution to cloud resolving modeling and to the GPM) and Dense GNSS Network [5].

2.1. Site Description

The ACONVEX site is located up-wind from Manaus-AM, Brazil, inside the campus of Embrapa Amazônia

Occidental, on Km-30 of AM-010 roadway. Although the area has been partially impacted by human activities, this is not of concern as most instruments are remote sensing devices. More importantly, internet connection and electricity from the power grid allows for remote operation of all instruments and reduces the maintenance visits to once a week. Figure 1 gives an overview of the site.



Figure 1: The location of ACONVEX site up-wind from Manaus-AM, Brazil, is indicated by the blue ballon. The red dot marks the position of the operational soundings.

Instruments installed include: a meteorological weather station, disdrometer, multi filter shadow band radiometer, cimel sun photometer (AERONET), vertical pointing radar, ceilometer and UV Raman Lidar.

2.2. UV Raman Lidar

The UV Raman Lidar is operational on the ACONVEX site since July 2011. It uses a Quantel CFR-400 Nd-YAG laser at 355 nm with 95 mJ per pulse and 10 Hz repetition rate. Beam is expanded by 3 and final laser divergence is 0.25 mrad. The optical system uses a bi-axial setup with a 400 mm separation between the cassegrain telescope and the laser axis. The telescope's primary mirror has 400 mm diameter and the secondary, 90 mm. Focal distance is 4000 mm resulting in a f 10 system. An iris is used at the focal plane which gives a FOV of 1.75 mrad and an initial overlap at 85 m and full overlap at 450 m.

No fiber optics are used and light passing through the iris goes directly in the optical detection box. Interferometric filters separate the elastic back scattered signal and the inelastic signals due to the raman crosssection of N₂ (387 nm) and H₂O (408 nm) which are read individually by Ramamatsu R988U-10 photo-multiplier-tubes. 355 and 387 nm are recorded in analog and photon-count modes, while 408 nm only in photon count. The geometry of the whole optical system developed by Raymetric Inc. is such that the signal density function on the cathode does not vary with the height of the detected signal. A neutral density filter is used to attenuate the elastic signal avoiding saturation, and a good signal to noise ratio is found up to 15 km depending on atmospheric conditions.

Fig. 2 shows typical measurements of inelastic channel in photon-count mode.

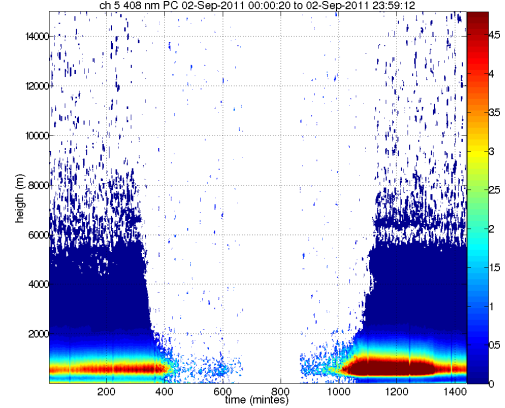


Figure 2: One day (1440 min) of 1-min acquisitions (600 shots) for inelastic H₂O photon-count channel is shown. Low signal to noise don't allow daytime measurements. Longer time averages increase s/n above 6 km. Data is from August 30th 2011.

The system is fully automated and includes a shutter controlled by the PLC clock to cover the telescope and laser quartz windows from direct sunlight exposure between 11 am and 2 pm local time. As a backup system a 10 mm shutter is positioned just above the iris and kept in its light-blocking position by a coil mechanism. Interlocks are connected to the UPS and to the sun light sensor, a small telescope with a 10° field of view around the large telescope axis. Environmental conditions effects on the electronics are minimized by continuously running an air conditioning and a dehumidifier inside the instrumentation cabinet.

3. WATER VAPOR MEASUREMENT

The lidar-raman equation for a pulse of wavelength λ returning at a raman wavelength λ' can be written as

$$P(z, \lambda, \lambda') = P_0 \frac{c\Delta T}{2} A_{tel} \eta_{eff}(\lambda') \frac{O(z)}{z^2} \beta(z, \lambda, \lambda') \exp \left[\int_0^z (\alpha(z', \lambda) + \alpha(z', \lambda')) dz' \right]$$

where P_0 is the pulse energy, $c\Delta T/2$ is its length, α is the volumetric attenuation coefficient, $\beta(z, \lambda, \lambda')$ is the raman backscatter coefficient, A_{tel} is the telescope effective area, $\eta_{eff}(\lambda')$ is the detection quantum efficiency, and $O(z)/z^{-2}$ is a geometric factor.

As the atmospheric concentration of N₂ is constant, it is possible to measure the concentration of H₂O by taking the ratio of both background corrected signals [7], what eliminates unknowns such as the geometrical factor. This is a well established technique [8] and result in the following expression

$$w_{H_2O} = C \Gamma_A \Gamma_M \frac{\overline{S_{H_2O}} - \overline{BG_{H_2O}}}{\overline{S_{N_2}} - \overline{BG_{N_2}}} \quad (1)$$

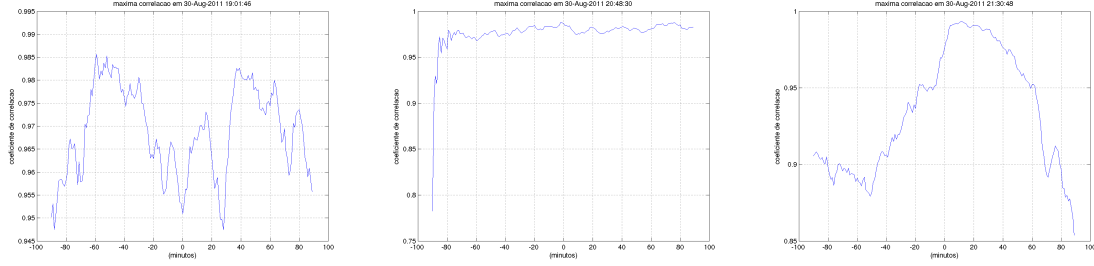


Figure 3: Panels show the lag correlation coefficient (500m-3km) between lidar profiles and reference water vapor measurements for: (left) SBMN standard levels only; (center) SBMN full resolution; (right) collocated sounding. Data from August 30th 2011.

where the constant Γ_A and Γ_M are the differential aerosol and molecular transmission between the N_2 and H_2O wavelengths and the overbars denote temporal and spatial averages necessary for obtaining a good signal to noise ratio.

There has been different approaches for treating the above equation. While some authors remove the contribution from both molecular and aerosol attenuation [7] from the calibration constant, some remove only the molecular part [9], and others make no correction [10]. While the first approach is more precise, it is also more difficult to implement operationally. In this work, the methodology of [10] is used and hence the derived calibration constants might include some contamination of the differential mie and rayleigh absorptions.

3.1. Calibration Constant

The calibration of Raman-Lidar systems for measurements of water vapor profiles is still a limiting factor [9]. Here the most common approach is used, i.e., a linear fit between the uncalibrated lidar profile and independent collocated soundings. Because radiosondes have an accuracy of about 5 to 10% in relative humidity, the calibration is performed below between 500m and 3 km where the accuracy is greater and where most water vapor is found.

The calibration process was divided in three steps: (1) temporal and vertical average of uncalibrated lidar profiles; (2) interpolation of high resolution lidar profiles to the sounding levels; and (3) linear regression between $w_{H_2O}^{sounding}$ and uncalibrated lidar profile. The temporal and vertical smoothing are necessary for obtaining a good signal to noise ratio, but care was taken not to smooth too much and remove real variations in the water profile. The time average was varied between 2 and 100 min, and between 15 to 75 m. The vertical correlation coefficient between 1 to 3 km was calculated for each profile between -1h and +1h of the launching time. The largest correlations were found at +8 min or ~ 2 km when using 2 min and 30 m averages (see Fig. 3).

Although collocated soundings are definitely the best approach for calibrating a lidar profile, one must agree that a calibration campaign to drop ones own radiosondes is

extremely time and money consuming and can only be done for a limited amount of time. Therefore, the calibration constant were obtained from only 8 collocated soundings performed during an intensive campaign in September 2011. For comparison, the calibration constant were also computed with the operational sounding performed twice a day, 30 km away in the Manaus military airport, the SBMN WMO station. In this case, two constants were calculated: (1) using only standard atmospheric levels as distributed via GTS; and (2) using full resolution, obtained from Brazil air-force. Only 8 operational soundings at 0Z were used, in the exact same nights as the collocated ones.

Figure 4 shows the fitting for the first day, a typical result. From left to right, results are SBMN at standard levels (aero); at all levels (SBMN); and the collocated sounding (RSsitio). Aero and SBMN give similar results, except for the larger 95% confidence level interval in the first case. Result from RSsitio are rather lower for this particular day and in general. Values of calibration constant averaged over all sounding were 0.878 ± 0.086 , 0.871 ± 0.058 and 0.681 ± 0.045 g/g.

4. DISCUSSION AND FUTURE WORK

Although previous works [9] have shown to be possible to calibrate a lidar water vapor profile from non-collocated sounding, our results indicates this is not possible for our particular case as the difference between the value of the calibration constant from collocated (0.681 ± 0.045 g/g) and non-collocated sounding (0.878 ± 0.086 and 0.871 ± 0.058) is statistically significant.

Figure 4 shows that the time series of the correlation between uncalibrated lidar profile and reference water vapor profile shows a maximum around 2 km only for the collocated sounding. For SBMN there is no clear pattern, what could be justified by different advection velocities on different layers and by the proximity of the sounding site to the river and city. The analysis of the vertical profile of the calibration constant, shown in 5, also indicates a behavior compatible with a differential advection between the 1 to 1.5 km and 1.5 to 2 km.

The uncertainty in the calibration constant obtained from collocated sounding, 0.681 ± 0.045 (rms) ± 0.040 (inst)

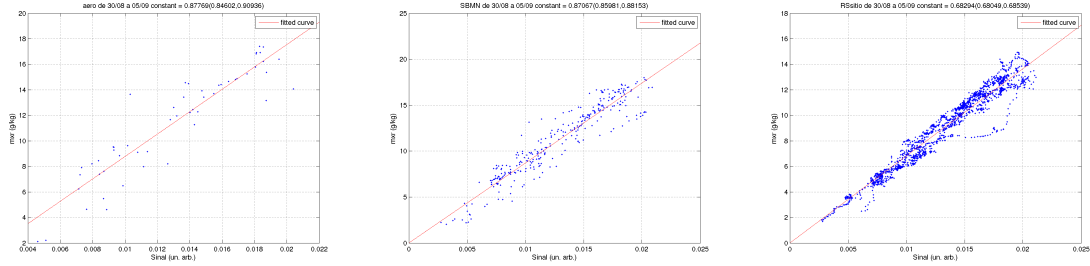


Figure 4: Panels show fitting between uncalibrated lidar profiles and reference water vapor measurements for: (left) SBMN standard levels only; (center) SBMN full resolution; (right) collocated sounding. Values between brackets are the 95% confidence limit. Data from August 30th 2011.

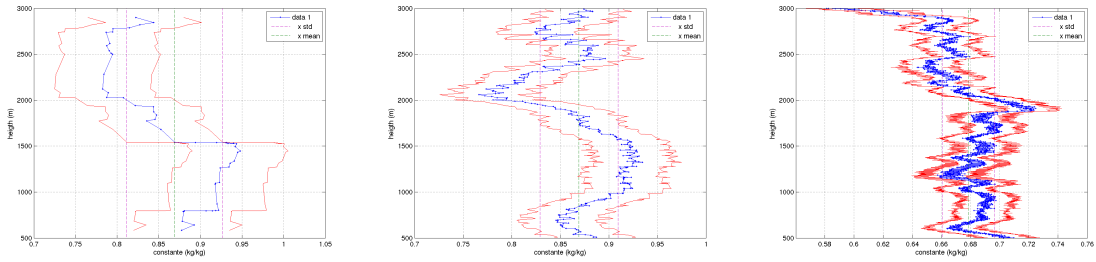


Figure 5: Panels show ratio between uncalibrated lidar profiles and reference water vapor measurements for: (left) SBMN standard levels only; (center) SBMN full resolution; (right) collocated sounding. Data shown is the average of 8 sounding between August 30th and September 5th 2011.

g/g, was about 6.6% rms between different sounding and 5.8% instrumental. Values are larger than the 2 to 6% range indicated by [11]. This indicates room for improvement. Currently, work is being done to remove the contribution of molecular and aerosol scattering from the calibration constant. This is probably particularly important for this region and this time of year, as September is the peak of the biomass burning season in the Amazon region.

ACKNOWLEDGMENTS

Author's acknowledge FAPESP's support under different research grants and thanks Dra. Rosa dos Santos/UEA-AM for being responsible for the radiosondes. Institutional support from EMBRAPA and LBA was fundamental. Dr. Barbosa is thankful for the instruments shared by AEROClima, CHUVA and GNNS Network projects.

REFERENCES

- Bretherton, C. and Smolarkiewicz, P. 1989: Gravity waves, compensating subsidence and detrainment around cumulus clouds. *J. Atmos. Sci.*, **46**, pp. 740.
- Holloway, C. and Neelin, J. 2009: Moisture vertical structure, column water vapor, and tropical deep convection. *J. Atmos. Sci.*, **66**, pp. 1665.
- Williams, E. and Renn, N. 1993: An analysis of the conditional instability of the tropical atmosphere. *Mon. Weath. Rev.*, **121**, pp. 21.
- Adams, D. and Souza, E. 2009: Cape and convective events over the southwest u.s. during the north american monsoon. *Mon. Weath. Rev.*, **137**, pp. 83.
- David K. Adams et al. 2011: A dense GNSS meteorological network for observing deep convection in the Amazon *Atmos. Sci. Lett.*. doi:10.1002/asl.312.
- Silva-Dias, M. et al. 2002: Cloud and rain processes in a biosphere-atmosphere interaction context in the amazon region. *J. Geo. Res.*, **107**(D20), 8072. doi:10.1029/2001JD000335.
- Whiteman, D.N. et al. 1992: Raman Lidar system for the measurement of water vapor and aerosols in the Earths atmosphere *Appl. Opt.*, **31**(16), pp. 3068.
- Melfi, S. H. 1972: Remote measurements of the atmosphere using Raman scattering *Appl. Opt.*, **11**, pp. 1288.
- D. Dionisi et al. 2010: Calibration of a Multichannel Water Vapor Raman Lidar through Noncollocated Operational Soundings: Optimization and Characterization of Accuracy and Variability *J. Atmos. Oceanic Technol.*, **27**, pp. 108.
- Bosser, P. et al. 2010: A case study of using Raman lidar measurements in high-accuracy GPS applications. *J. Geod.*, **84**, pp. 251. doi:10.1007/s00190-009-0362-x.
- Revercomb, H.E. et al. 2003: The ARM programs water vapor intensive observation periods *BAMS*, **84**(2), pp. 217. doi:10.1175/BAMS-84-2-217.